HHS Public Access

Author manuscript

J Neuropsychiatry Clin Neurosci. Author manuscript; available in PMC 2023 March 16.

Published in final edited form as:

J Neuropsychiatry Clin Neurosci. 2020 ; 32(4): 370–375. doi:10.1176/appi.neuropsych.19070165.

Topography of Cholinergic Changes in Dementia with Lewy Bodies Involves Key Neural Network Hubs

Prabesh Kanel, PhD[1,4], **Martijn L.T.M. Müller, PhD**[1,4], **Sygrid van der Zee, MS**[5], **Carlos A. Sanchez-Catasus, PhD**[1,4], **Robert A. Koeppe, PhD**[1], **Kirk A. Frey**[1,2], **Nicolaas I. Bohnen, MD, PhD**[1,2,3,4]

[1]Department of Radiology, University of Michigan, Ann Arbor, MI, United States, 48104

[2]Department of Neurology, University of Michigan, Ann Arbor, MI, United States, 48104

[3]Neurology Service and GRECC, Veterans Administration Ann Arbor Healthcare System, Ann Arbor, MI, United States, 48104

[4]Morris K. Udall Center of Excellence for Parkinson's Disease Research, University of Michigan, Ann Arbor, MI, United States.

[5]Department of Neurology, University of Groningen, University Medical Center Groningen, Groningen, the Netherlands.

Abstract

OBJECTIVES: To investigate the topography of cholinergic vulnerability in patients with dementia with Lewy bodies (DLB) using PET imaging with the vesicular acetylcholine transporter (VAChT) ^{18}F-fluoroethoxybenzovesamicol (^{18}F-FEOBV) radioligand.

METHODS: Group comparison study of five participants with DLB and 21 normal control elderly who underwent clinical assessment and ^{18}F-FEOBV PET imaging.

RESULTS: Compared to the control group, reduced VAChT binding in DLB patients demonstrated non-diffuse regionally distinct and prominent reductions in bilateral opercula and anterior-to-mid cingulate cortices, bilateral insula, right more than left lateral geniculate nuclei, pulvinar, right proximal optic radiation, bilateral anterior and superior thalami, and posterior hippocampal fimbria and fornices.

CONCLUSIONS: The topography of cholinergic vulnerability in DLB involves key hubs involved in tonic alertness (cingulo-opercular), saliency (insula), visual attention (visual thalamus), and spatial navigation (fimbria/fornix) networks. The distinct denervation pattern suggests an important cholinergic role in specific clinical disease-defining features, like cognitive fluctuations,

Corresponding author: Prabesh Kanel, PhD, Department of Radiology, University of Michigan, Functional Neuroimaging, Cognitive and Mobility Laboratory, 24 Frank Lloyd Wright Drive, Box 362, Ann Arbor, MI 48105-9755, TEL: (1) 734 998 6694; FAX: (1) 734 998 8403. prabeshk@umich.edu.

Relevant conflicts of interest/financial disclosures:
The authors have no relevant financial or conflict of interest to disclose.

Manuscript disclose: FEOBV PET data from a subset of the participants in this study were previously reported in a FEOBV PET methods paper (1). The current manuscripts is based on the previously described PET quantification method but has a different (i.e., voxel-based) group PET comparison approach that allows subregional granular brain assessment.

visuoperceptual causing visual hallucinations, visuospatial changes, and loss of balance caused by DLB.

Keywords

Acetylcholine; cingulo-opercular network; cognition; dementia with Lewy bodies; saliency; visual thalamus

Introduction

The cholinergic system plays an important role in human cognition and evidence of degeneration of this system has been reported by post-mortem and *in vivo* imaging studies in neurodegenerative disorders, esp. Alzheimer's disease and dementia with Lewy bodies (DLB).

The cerebral cholinergic system that involves in the regulation of attention and higher-order cognitive processing are grouped into 8 distinct nuclear groups (labeled as cholinergic groups Ch1–8) based on the efferent projection to their anatomical targets. Efferents from the Ch1 (medial septal nucleus) and Ch2 (vertical limb of the diagonal band of Broca) provide major innervation for the hippocampus via the fornix; Ch3 (horizontal limb of the diagonal band of Broca) provides innervation for the olfactory bulb; Ch4 (Nucleus basalis of Meynert) delivers major cholinergic input to neocortical mantle and amygdala; and Ch5–6 (pedunculopontine and laterodorsal tegmental nucleus) provides cholinergic projections to the thalamus, basal ganglia, basal forebrain, other brainstem structures, and spinal cord (1–4). Efferents from Ch7 (medial habenula) and Ch8 (parabigeminal nucleus) provide innervation for the interpeduncular nucleus and superior colliculus, respectively (3). As these systems support a number of cognitive, neurobehavioral and motor functions, cholinergic losses are thought to play an important role in cognitive and neurobehavioral changes in AD, Parkinson's disease (PD) and DLB (5–8). We have previously shown that cortical (Ch4) cholinergic losses were more severe in Lewy body dementia (DLB and PD dementia) compared to AD and PD without dementia (9) and found to correlate with the degree of cognitive impairment (7). It is plausible that the earlier manifestation of neurobehavioral symptoms in DLB compared to AD may -in part- reflect more severe or more extensive cholinergic losses that are not limited to cortical but also subcortical changes (1).

Characterizing the severity and topographic extent of cholinergic denervation in DLB may provide better insight in the relationship between cholinergic system changes and clinical manifestations, such as cognitive fluctuations, attentional deficits, visuospatial and visuoperceptual changes, visual hallucinations or falls in DLB (10, 11). *In vivo* brain imaging studies of DLB have shown nigrostriatal dopaminergic and more diffuse brain cholinergic losses (12). However, a limitation of prior cholinergic imaging studies in DLB involves the use of either global cortical or large lobar volume-of-interests (VOI) to characterize cholinergic innervation changes in this disorder. This may result in missed recognition of small-sized regional cholinergic changes due to dilution when computing average brain binding changes in large lobar or global cortical VOIs. The

purpose of this study is to explore a more granular topographic assessment of regional cholinergic binding differences between DLB and control subjects using a spatially non-biased whole brain voxel-based analysis of vesicular acetylcholine transporter (VAChT) ^{18}F-fluoroethoxybenzovesamicol (^{18}F-FEOBV) PET imaging. We hypothesize that cholinergic brain changes are not mainly globally diffuse, but that cholinergic denervation changes in DLB may be driven also by regional brain functionality. We report findings of ^{18}F-FEOBV PET obtained in five DLB participants and in 21 control subjects. ^{18}F-FEOBV whole brain and volume-of-interest PET data from a subset of these participants has been previously reported in a FEOBV PET quantification Letter to the Editor (1).

Subjects and Methods

Subjects

The patients were recruited at the Cognitive Disorders Clinic at the University of Michigan Health system. Third international clinical diagnostic consensus criteria were used to diagnose probable DLB (13). The control group was collected from our poll of the existing normal control elderly PET database that matched with our patients' age and gender. At the time of the PET scans, the normal controls had a normal neurological examination with no history of neurological or psychiatric diseases. Any participants that had evidence of large vessel strokes or other intracranial lesions were excluded from the current study. Written informed consent (or assent) was collected from the participant (or legal representative) before study participation. The study was approved by the University of Michigan Medical IRB and in compliance with the Declaration of Helsinki guidelines. All subjects underwent brain MRIs and delayed acquisition (3–3.5 hours, scanned every 5 minutes for a total of 6 frames) ^{18}F-FEOBV (bolus i.v of 8 mCi) PET. T1-weighted imaging was performed on a 3 Tesla Philips Achieva system (Philips, Best, The Netherlands). A three-dimensional (3D) inversion recovery-prepared turbo field echo was performed in the sagittal plane using repetition time/echo time/inversion time = 9.8/4.6/1041 ms; turbo factor = 200; single average; field of view (FOV) = 240 × 200 × 160 mm; acquired matrix = 240 × 200 × 160 slices; and reconstructed to 1-mm isotropic resolution. PET imaging was performed in 3D imaging mode with a Siemens ECAT Exact HR+ tomograph, as previously reported (14). ^{18}F-FEOBV was prepared in high radiochemical purity (>95%) (15). Delayed dynamic imaging was performed over 30 minutes (in six 5-minute frames) starting 3 hours after an intravenous bolus dose injection of 8 mCi ^{18}F-FEOBV**(3).** The PET imaging frames were spatially coregistered within-subjects with a rigid-body transformation to reduce the effects of subject motion during the imaging session.

Spatial preprocessing

Freesurfer software suite (https://surfer.nmr.mgh.harvard.edu) was used to create a supratentorial white matter mask. The mask included only voxels from the Freesurfer white matter segmentation that was above the ventricle. The mask was further eroded using a morphological filter to avoid partial volume effects from the cortical areas and include only the core voxels of supratentorial white matter voxels. The remaining voxels after this procedure were the reference region. The mean image from the six delayed imaging frames was normalized using the reference region to create parametric images that reflected

the distribution volume ratios (DVR) (1). All parametric PET images and the registered structural MR images were processed using high-dimensional DARTEL registration, spatial normalization to a template space in Montreal Neurological Institute (MNI) space, and segmentation into gray matter, white matter and cerebrospinal fluid using the SPM12 software package (https://www.fil.ion.ucl.ac.uk/spm/). The parametric PET images were corrected for partial volume effects using the Muller-Gartner (16) method before being normalized into MNI space. The normalized images were spatially smoothed (FWHM = 8 mm) to remove random noise.

Statistical Analysis

Group comparison of demographic and clinical data of the DLB and normal control subjects was performed using Student *t* or Chi square testing (with the group classification being the independent variable and the demographic and clinical measures dependent variables). Using SPM12, we applied voxel-based two sample t-test comparing the corrected and spatially normalized parametric images between groups. The between-group statistical parametric mapping results were thresholded at voxel level ($p<0.001$) and corrected for whole-brain comparisons using peak-level false discovery rate ($p<0.005$). Clusters that survived the peak-level false discovery rate were interpreted as significant.

Results

This cross-sectional study consisted of 5 participants with DLB (three females; two males), with an average age of 77.8±4.2 years and a duration of disease of 4.5±2.1 years (median = 6; range = 4), and a Mini-Mental State Exam (17) score of 18.6±4.8. Table 1 lists the core clinical criteria of the participants with DLB.

Demographic and clinical information for the DLB and control group is presented in Table 2. Twenty-one normal control elderly studied consisted of 13 females and 8 males with an average age 73.5±8.5 years and Mini-Mental State Exam score of 28.67±1.35.

Results of the voxel-based comparison between the DLB and control group are shown in Figure 1. There were significant cholinergic binding reductions in the DLB compared to the control group in the following areas: the bilateral opercula, anterior-to-mid cingulate cortices, bilateral insula, right more than left lateral geniculate nuclei, pulvinar, right proximal optic radiation, bilateral anterior and superior thalami, and bilateral posterior hippocampal fimbria and fornices. Table 3 lists the main clusters and their peak MNI coordinates and associated network hubs. We repeated this analysis with years of education included as a covariate. This analysis yielded similar results (see Supplemental Figure 1).

Exploratory post-hoc cognitive correlation analysis

We performed an exploratory voxel-based regression analysis of the PET data and the MMSE as outcome parameter within the group of the DLB participants. Results are shown in supplemental Figure 2. Clusters (uncorrected $P<0.05$) were seen in the following regions: bilateral lateral geniculate nucleus, bilateral lingual gyri/optic radiations, left medial occipital, left superior posterior parietal, right superior parietal, right posterior frontal, and right superior temporal cortices and the right hippocampus. No clusters meeting this

criterion were found in a similar voxel-based PET-MMSE regression analysis in the normal control group.

Discussion

Voxel-based whole brain analysis of VAChT PET identified a distinct topographic cholinergic denervation pattern rather than diffuse cerebral losses in DLB compared to the elderly control group. Regions showing cholinergic denervation overlapped with key hubs of neural networks responsible for visual attention (visual thalamus) (18), salience (insula) (19), spatial navigation (fimbria/fornix) (20), and maintenance of alertness (cingulo-opercular) networks (21). Specifically, we found cholinergic changes in the following hubs of each network: Maintenance of alertness (cingulo-opercular) network: insula, operculum, cingulum, thalamus; Salience network: anterior insula, anterior cingulum; Visual attention network: visual thalamus, including the lateral geniculate nucleus; Spatial navigation network: fornix, fimbria, hippocampus, and anterior thalamus.

Graph theory analysis of functional connectivity resting state MRI identified two distinct top-down task-control networks (22, 23). The dorsolateral prefrontal cortex and intraparietal sulcus are hubs within the frontoparietal task control (FPTC) network. The FPTC network is important for start-cue and error-related activity and may initiate and adapt control on a more rapid and trial-by-trial basis. The cingulo-opercular task control (COTC) network encompasses medial superior frontal cortex, dorsal anterior cingulate, frontal operculum, anterior insula and thalamic regions (22). Effectively, the COTC graph may include parts of both the large-scale distributed network of the cingulo-opercular and salience networks (23). The topography of cholinergic reductions in our DLB patients suggests preferential cholinergic involvement of the COTC. The COTC network controls the goal-directed behavior more on a set maintenance mode using a longer duration time scale, such as needed for maintaining alertness. Clinically, this may be reflected in a lack of maintenance of a functional operative state and difficulties staying on task in DLB persons in their daily life functions resulting in cognitive fluctuations. Our findings are also compatible with the emerging notion of an important role of the cingulo-opercular network in task-switching from a passive task to an active task (24).

Another interesting observation was the asymmetry of visual thalamic regions findings, such as right more than left lateral geniculate nuclei, pulvinar, and right proximal optic radiation changes. These findings may reflect associations with the ventral attention network, which has a right-hemispheric dominance (25). The ventral attention network is involved in the detection of ‘bottom-up’ salient and behaviorally relevant stimuli in the environment, especially when the stimuli are initially unattended. This network is highly integrated with the visual system and includes the ventral part of the supramarginal gyrus, ventral frontal cortex, posterior part of the superior temporal sulcus and gyrus, inferior frontal gyrus, middle frontal gyrus, frontal operculum, and anterior insula, which acts as a “network breaker” that interrupts attention in the dorsal system and reorients attention towards stimulus-driven object (26). These observations agree with our previous findings that lower cholinergic activity in the thalamus was associated with decreased saliency processing in patients with Parkinson’s disease (27). This is likely mediated by the right lateral geniculate

nucleus where decreased cholinergic innervation may be associated with compromised visual attention, perceptual abnormalities and possibly hallucinations in patients with DLB. We also recently reported on an association between reduced cholinergic integrity of the right lateral geniculate nucleus and falls in patients with PD (28). A similar association may exist in patients with DLB; however, this will require further confirmation.

The hippocampus plays an important role in spatial navigation (20), which is a key function for safely walking. Our findings show evidence of reduced cholinergic transporter binding in the hippocampal fimbria and fornices. Cholinergic deficits in these regions may possibly compromise the integration of cognitive and sensorimotor functions while walking. Clinically, these regional deficits may hypothetically be associated with the wandering behavior in the DLB patients.

Exploratory findings of a voxel-based whole brain regression analysis of the cholinergic PET data and using the MMSE as the outcome parameter showed several clusters that overlapped with several of the topographic cholinergic denervation regions. A notable finding was involvement of the visual system, especially the bilateral lateral geniculate nuclei and adjacent visual lobe regions. This may possibly be associated with visual processing dependent cognitive and/or neurobehavioral changes in DLB. Other regions showed overlap with the COTC and spatial navigation networks.

No clusters meeting this criterion were found for a similar analysis in the normal control group suggesting disease-specific cognitive correlates in the DLB group. These preliminary findings need to be confirmed in a larger sample size.

Identification of neural network changes underlying the clinical symptom manifestations in patients with DLB would augur network neurostimulation approaches as a complementary treatment strategy to existing pharmacological and behavioral interventions. Furthermore, our study has identified hubs of key neural networks that may contribute to the clinical symptom manifestation of DLB. Future studies comparing directly *in vivo* imaging findings with post-mortem data may be very informative to advance our understanding of the neurodegenerative mechanisms underlying DLB. For example, findings of cholinergic changes in the lateral geniculate nucleus in DLB are very novel but at present there is a critical gap of knowledge to explain the cholinergic vulnerability of the lateral geniculate nucleus in DLB. Another topic of future *in vivo-ex vivo* correlation research would be to assess for pathological changes in hubs corresponding to regional network vulnerability in post-mortem data.

There are several limitations of this study. One limitation of the study is the small sample size. Further studies using a larger sample sizes are needed to validate these topographic VAChT findings and associate them with clinical symptoms. The second limitation is the cross-sectional design that lacks longitudinal information about the cholinergic binding areas and how cholinergic vesicular transporters may change in relationship to the temporal manifestation of specific clinical symptoms. Thirdly, we do not have detailed neuropsychological testing data to validate the clinical diagnosis of probable DLB. Lastly, our neural network interpretation of the topography of neuroimaging data in the absence

of neuropsychological metrics, functional MRI or electrophysiological measures remains speculative.

We conclude that cholinergic changes are not diffuse in DLB but have a topographical distinct pattern of vulnerability that overlaps with hubs of important large-scale functional networks. Therefore, cholinergic network changes may explain some of the disease-defining features of DLB.

Supplementary Material

Refer to Web version on PubMed Central for supplementary material.

Acknowledgment:

This work was supported by NIH grants P01 NS015655, RO1 NS070856 & P50 NS091856.

Disclosures

Dr. Kanel has nothing to disclose.

Dr. Muller has research support from the NIH, Michael J. Fox Foundation and the Department of Veteran Affairs.

Ms. Van der Zee has nothing to disclose.

Dr. Sanchez-Catasus has nothing to disclose.

Dr. Koeppe has received grant support from the NIH.

Dr. Frey has research support from the NIH, GE Healthcare and AVID Radiopharmaceuticals (Eli Lilly subsidiary). Dr. Frey also serves as a consultant to AVID Radiopharmaceuticals, MIMVista, Inc, Bayer-Schering and GE healthcare. He also holds equity (common stock) in GE, Bristol-Myers, Merck and Novo-Nordisk.

Dr. Bohnen has research support from the NIH, Department of Veteran Affairs, the Michael J. Fox Foundation, Eisai,and EIP Pharma.

Author's Roles:

Dr. Kanel: Analysis and interpretation; manuscript preparation.

Dr. Müller: Acquisition of data; Study supervision; Analysis and interpretation; Critical revision.

Ms. Van der Zee: Critical revision of the manuscript for important intellectual content.

Dr. Sanchez-Catasus: Critical revision of the manuscript for important intellectual content.

Dr. Koeppe: Acquisition of data; Critical revision of the manuscript for important intellectual content.

Dr. Frey: Obtained funding; Study supervision; Critical revision of the manuscript for important intellectual content.

Dr. Bohnen: Obtained funding; Acquisition of data; Study supervision; Analysis and interpretation; manuscript preparation.

References

1. Nejad-Davarani S, Koeppe RA, Albin RL, Frey KA, Muller M, Bohnen NI. Quantification of brain cholinergic denervation in dementia with Lewy bodies using PET imaging with [(18)F]-FEOBV. Molecular psychiatry. 2019;24(3):322–7. [PubMed: 30082840]

2. Mesulam MM. Cholinergic circuitry of the human nucleus basalis and its fate in Alzheimer's disease. The Journal of comparative neurology. 2013;521(18):4124–44. [PubMed: 23852922]
3. Arciniegas DB. Cholinergic dysfunction and cognitive impairment after traumatic brain injury. Part 1: the structure and function of cerebral cholinergic systems. The Journal of head trauma rehabilitation. 2011;26(1):98–101. [PubMed: 21209567]
4. Selden NR, Gitelman DR, Salamon-Murayama N, Parrish TB, Mesulam MM. Trajectories of cholinergic pathways within the cerebral hemispheres of the human brain. Brain. 1998;121 (Pt 12):2249–57. [PubMed: 9874478]
5. Pinto T, Lanctot KL, Herrmann N. Revisiting the cholinergic hypothesis of behavioral and psychological symptoms in dementia of the Alzheimer's type. Ageing research reviews. 2011;10(4):404–12. [PubMed: 21292041]
6. Perry EK, Curtis M, Dick DJ, Candy JM, Atack JR, Bloxham CA, et al. Cholinergic correlates of cognitive impairment in Parkinson's disease: comparisons with Alzheimer's disease. Journal of neurology, neurosurgery, and psychiatry. 1985;48(5):413–21. [PubMed: 3998751]
7. Bohnen NI, Kaufer DI, Hendrickson R, Ivanco LS, Lopresti BJ, Constantine GM, et al. Cognitive correlates of cortical cholinergic denervation in Parkinson's disease and parkinsonian dementia. J Neurol. 2006;253(2):242–7. [PubMed: 16133720]
8. Hilker R, Thomas AV, Klein JC, Weisenbach S, Kalbe E, Burghaus L, et al. Dementia in Parkinson disease: functional imaging of cholinergic and dopaminergic pathways. Neurology. 2005;65(11):1716–22. [PubMed: 16344512]
9. Bohnen NI, Kaufer DI, Ivanco LS, Lopresti B, Koeppe RA, Davis JG, et al. Cortical cholinergic function is more severely affected in parkinsonian dementia than in Alzheimer disease: an in vivo positron emission tomographic study. Archives of neurology. 2003;60(12):1745–8. [PubMed: 14676050]
10. McKeith IG, Boeve BF, Dickson DW, Halliday G, Taylor JP, Weintraub D, et al. Diagnosis and management of dementia with Lewy bodies: Fourth consensus report of the DLB Consortium. Neurology. 2017;89(1):88–100. [PubMed: 28592453]
11. McKeith IG, Wesnes KA, Perry E, Ferrara R. Hallucinations predict attentional improvements with rivastigmine in dementia with lewy bodies. Dementia and geriatric cognitive disorders. 2004;18(1):94–100. [PubMed: 15087584]
12. Bohnen NI, Muller M, Frey KA. Molecular Imaging and Updated Diagnostic Criteria in Lewy Body Dementias. Current neurology and neuroscience reports. 2017;17(10):73. [PubMed: 28808912]
13. Ballard C, Ziabreva I, Perry R, Larsen JP, O'Brien J, McKeith I, et al. Differences in neuropathologic characteristics across the Lewy body dementia spectrum. Neurology. 2006;67(11):1931–4. [PubMed: 17159096]
14. Bohnen NI, Muller ML, Kotagal V, Koeppe RA, Kilbourn MR, Gilman S, et al. Heterogeneity of cholinergic denervation in Parkinson's disease without dementia. Journal of cerebral blood flow and metabolism : official journal of the International Society of Cerebral Blood Flow and Metabolism. 2012;32(8):1609–17. [PubMed: 22569194]
15. Shao X, Hoareau R, Hockley BG, Tluczek LJ, Henderson BD, Padgett HC, et al. Highlighting the Versatility of the Tracerlab Synthesis Modules. Part 1: Fully Automated Production of [F]Labelled Radiopharmaceuticals using a Tracerlab FX(FN). Journal of labelled compounds & radiopharmaceuticals. 2011;54(6):292–307. [PubMed: 21769163]
16. Muller-Gartner HW, Links JM, Prince JL, Bryan RN, McVeigh E, Leal JP, et al. Measurement of radiotracer concentration in brain gray matter using positron emission tomography: MRI-based correction for partial volume effects. Journal of cerebral blood flow and metabolism : official journal of the International Society of Cerebral Blood Flow and Metabolism. 1992;12(4):571–83. [PubMed: 1618936]
17. Folstein MF, Folstein SE, McHugh PR. "Mini-mental state". A practical method for grading the cognitive state of patients for the clinician. Journal of psychiatric research. 1975;12(3):189–98. [PubMed: 1202204]
18. Saalmann YB, Kastner S. Cognitive and perceptual functions of the visual thalamus. Neuron. 2011;71(2):209–23. [PubMed: 21791281]

19. Menon V, Uddin LQ. Saliency, switching, attention and control: a network model of insula function. Brain structure & function. 2010;214(5–6):655–67. [PubMed: 20512370]
20. Sutherland RJ, Rodriguez AJ. The role of the fornix/fimbria and some related subcortical structures in place learning and memory. Behavioural brain research. 1989;32(3):265–77. [PubMed: 2496702]
21. Coste CP, Kleinschmidt A. Cingulo-opercular network activity maintains alertness. NeuroImage. 2016;128:264–72. [PubMed: 26801604]
22. Dosenbach NU, Fair DA, Cohen AL, Schlaggar BL, Petersen SE. A dual-networks architecture of top-down control. Trends in cognitive sciences. 2008;12(3):99–105. [PubMed: 18262825]
23. Power JD, Cohen AL, Nelson SM, Wig GS, Barnes KA, Church JA, et al. Functional network organization of the human brain. Neuron. 2011;72(4):665–78. [PubMed: 22099467]
24. Sadaghiani S, D'Esposito M. Functional Characterization of the Cingulo-Opercular Network in the Maintenance of Tonic Alertness. Cerebral cortex (New York, NY : 1991). 2015;25(9):2763–73.
25. Shulman GL, Pope DL, Astafiev SV, McAvoy MP, Snyder AZ, Corbetta M. Right hemisphere dominance during spatial selective attention and target detection occurs outside the dorsal frontoparietal network. The Journal of neuroscience : the official journal of the Society for Neuroscience. 2010;30(10):3640–51. [PubMed: 20219998]
26. Corbetta M, Shulman GL. Control of goal-directed and stimulus-driven attention in the brain. Nature reviews Neuroscience. 2002;3(3):201–15. [PubMed: 11994752]
27. Kim K, Muller M, Bohnen NI, Sarter M, Lustig C. Thalamic cholinergic innervation makes a specific bottom-up contribution to signal detection: Evidence from Parkinson's disease patients with defined cholinergic losses. NeuroImage. 2017;149:295–304. [PubMed: 28167350]
28. Bohnen NI, Kanel P, Zhou Z, Koeppe RA, Frey KA, Dauer WT, et al. Cholinergic system changes of falls and freezing of gait in Parkinson's disease. Annals of neurology. 2019;85(4):538–49. [PubMed: 30720884]

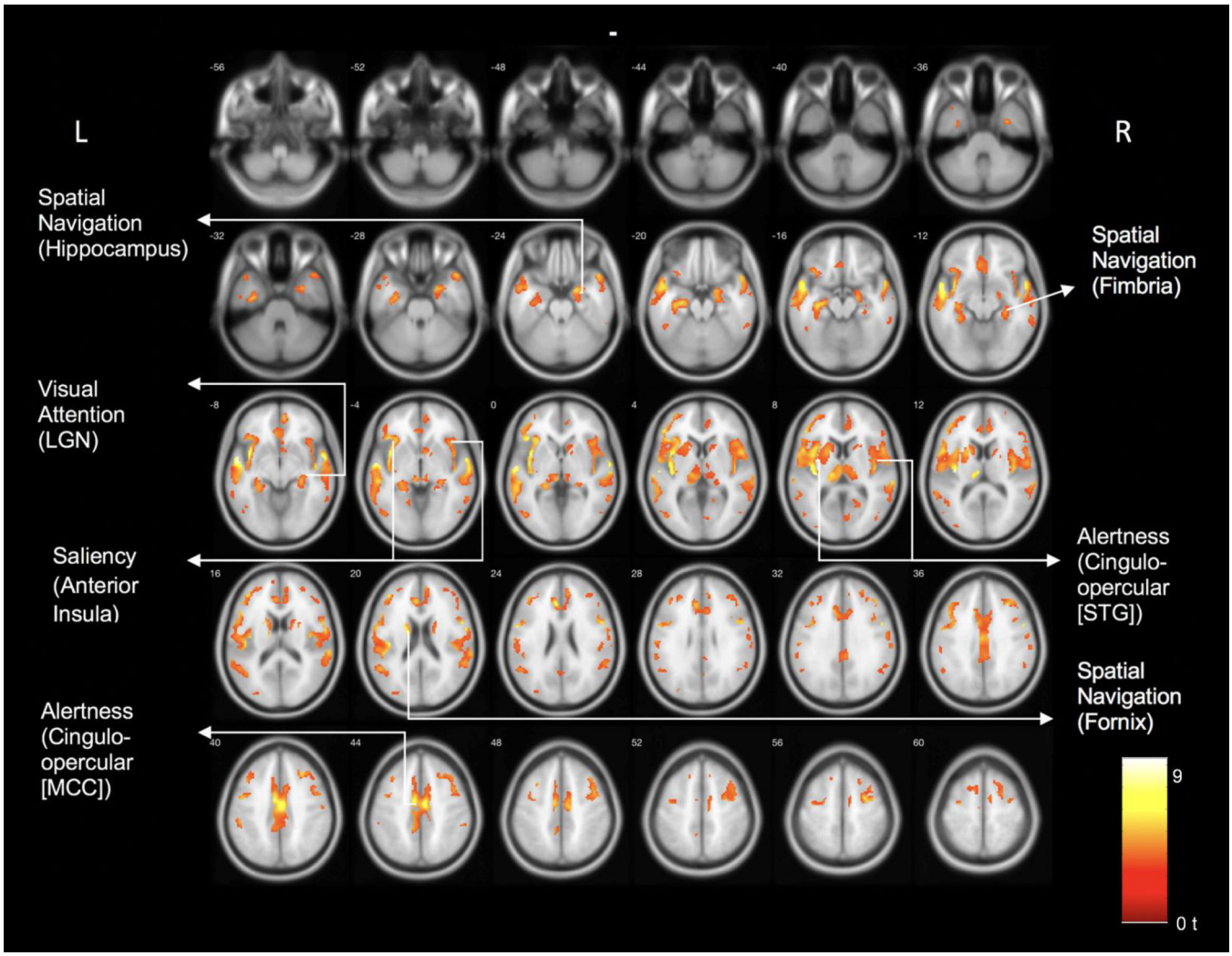

Figure 1. Clusters of reduced cholinergic binding in dementia of Lewy bodies (DLB)[a]

[a] The image shows a statistical parametric voxel-based analysis of VAChT binding compared to normal controls projected on a mean normalized structural image (MNI) in the axial plane.

Results show reductions in key areas associated with visual attention (visual thalamus), salience (insula), spatial navigation (fimbria/fornix), and alertness (cingulo-opercular) networks.

Table 1:

Demographic and Clinical information of participants with DLB

Subject	DLB1	DLB2	DLB3	DLB4	DLB5
Age, years	75	75	78	76	85
Gender	f	f	m	m	F
Duration, years	2.5	2	6	6	6
MMSE	24	19	12	16	22
Fluctuations	Yes	Yes	Yes	Yes	Yes
Hallucinations	No	No	Yes	Yes	Yes
Parkinsonism	Yes	Yes	No	Yes	Yes
Medication	Donepezil,carbidopa-levodopa, citalopram, buspirone	donepezil, carbidopa-levodopa	clonazepam, memantine, quetiapine	donepezil, carbidopa-levodopa, quetiapine	donepezil, venlafaxine

Table 2.

Demographic group differences between the DLB group[a] and the healthy comparator group[b]

	DLB		Control group		Value	Significance
	M	SD	M	SD		
Age, years	77.8	4.2	73.62	8.37	t=−1.072[c]	0.294
MMSE	18.6	4.8	28.67	1.35	t=4.670[c]	0.009
Gender	N/A		N/A		χ^2=0.006[d]	0.937
Education, years	11.8	0.45	17.62	2.33	t=5.468[c]	0.000

[a]The male/female ratio was 2/3

[b]The male/female ratio was 8/13

[c]t-value

[d]Pearson Chi Square value

Table 3.

Significant clusters with reduced cholinergic binding in dementia with Lewy bodies (DLB) compared to normal elderly

Cluster[a] (voxels)	p-value[b]	Peak MNI Coordinates			z-value	t-value	Peak Voxel location[c]	Predominant Network Hub[d]
		X	Y	Z				
2172	p<0.001	−28	−18	18	4.84	6.18	Left Hippocampus peak with cluster extending into LGN	Spatial Navigation & Visual Attention networks
6116	p<0.001	−58	−6	−4	6.24	9.482	Left BA22 peak with cluster extending into insula	Cingulo-opercular & Saliency networks
7726	p<0.001	52	4	34	5.50	7.566	Right BA6 peak with cluster extending into insula	Cingulo-opercular & Saliency networks
274	p<0.001	−4	32	−8	3.90	4.642	Left BA32 (Anterior cingulum)	Cingulo-opercular network
213	p<0.001	19	2	18	3.91	4.684	Right Caudate with cluster extending into fornix	Spatial Navigation network

[a] Significant cluster extending to key areas.

[b] Corrected peak-wise false discovery rate (FDR).

[c] brain region with peak t-values and the extending key regions for that cluster.

[d] Key large scale neural network hubs that overlap with the significant clusters.

BA: Brodmann area; LGN: Lateral geniculate nucleus; MNI: Montreal Neurological Institute.